ELSEVIER

Biophysical Chemistry 125 (2007) 298–305

Biophysical Chemistry

http://www.elsevier.com/locate/biophyschem

Translational and rotational motions of proteins in a protein crowded environment

Silvia Zorrilla [a], Mark A. Hink [b], Antonie J.W.G. Visser [b], M. Pilar Lillo [a,*]

[a] *Instituto de Química Física "Rocasolano", Consejo Superior Investigaciones Científicas (CSIC), Serrano 119, 28006 Madrid, Spain*
[b] *MicroSpectroscopy Centre, Laboratory of Biochemistry, Wageningen University, P.O. Box 8128, 6700 ET Wageningen, The Netherlands*

Received 2 August 2006; received in revised form 6 September 2006; accepted 6 September 2006
Available online 27 September 2006

Abstract

Fluorescence correlation spectroscopy (FCS) was used to measure the translational diffusion of labeled apomyoglobin (tracer) in concentrated solutions of ribonuclease A and human serum albumin (crowders), as a quantitative model system of protein diffusive motions in crowded physiological environments. The ratio of the diffusion coefficient of the tracer protein in the protein crowded solutions and its diffusion coefficient in aqueous solution has been interpreted in terms of local apparent viscosities, a molecular parameter characteristic for each tracer–crowder system. In all protein solutions studied in this work, local translational viscosity values were larger than the solution bulk viscosity, and larger than rotational viscosities estimated for apomyoglobin in the same crowding solutions. Here we propose a method to estimate local apparent viscosities for the tracer translational and rotational diffusion directly from the bulk viscosity of the concentrated protein solutions. As a result of this study, the identification of protein species and the study of hydrodynamic changes and interactions in model crowded protein solutions by means of FCS and time-resolved fluorescence depolarization techniques may be expected to be greatly simplified.

Keywords: Translational diffusion; Rotational diffusion; FCS; Macromolecular crowding

1. Introduction

Macromolecules occupy a substantial fraction (between 10% and 30%) of the total volume in physiological systems [1–3]. Such crowded environments might hinder the diffusion of biomolecules involved in crucial biological processes: metabolisms, transport of solutes, protein processing and signaling events, and may have large effects on their reaction rates and apparent equilibrium constants [4–8]. It is therefore important to incorporate crowding effects in the design and interpretation of *in vitro* studies [9,10], in order appropriately to understand and quantify how kinetic properties of specific macromolecules in physiological media are modified by the presence of other, neutral (non-interacting) macromolecules in their neighborhood. Among other biophysical techniques, methods based on fluorescence spectroscopy [11–13] appear to be very convenient for interaction studies in crowded media due to the possibility of specifically labeling only the tracer protein with extrinsic fluorescent dyes, which in this way can be distinguished easily from the crowding macromolecules. These techniques allow characterization and quantification of the hydrodynamic properties of free and bound species, both in crowded model solutions [14,15] and in whole living cells [6,16–18], using their fluorescence. Time-resolved fluorescence depolarization (TRFD) measurements provide a detailed description of the rotationally depolarizing motions of the tracer molecules that take place on the nanosecond time scale. Fluorescence correlation spectroscopy (FCS) measures translational diffusion times by autocorrelation analysis of fluctuations in the fluorescence intensity collected from a small group of diffusing molecules in an open sample volume element [19,20]. In (infinitely) dilute solutions, the rotational (D_r^0) and translational (D_t^0) diffusion coefficients are related to the hydrodynamic radius (R_T) of the labeled biomolecule (tracer), and to the absolute temperature (T) and viscosity (η) of the solution, through the Stokes–Einstein–Debye (SED) and the Stokes–Einstein (SE) relationships respectively [21–23], which assume that, in terms of its resistance to Brownian rotations or translations, the solvent behaves as a viscous continuum. However, the complexity of cellular

* Corresponding author. Tel.: +34 915619400; fax: +34 915642431.
E-mail address: pilar.lillo@iqfr.csic.es (M.P. Lillo).

0301-4622/$ - see front matter © 2006 Elsevier B.V. All rights reserved.
doi:10.1016/j.bpc.2006.09.003

systems makes the proper interpretation of kinetic data challenging, since the SE and SED relationships are not directly applicable to tracer molecule diffusion in these media. As a first approximation, however, it may be useful to generalize the SE and SED relations with η replaced by the *local apparent viscosity* or *equivalent viscosity* [24], an effective molecular parameter which would include all the neighboring effects of the crowder molecules upon the rotational (η_r) and translational (η_t) motions of the tracer in crowded media:

$$D_r = kT/(8\pi\eta_r R_T^3); \qquad D_t = kT/(6\pi\eta_t R_T) \tag{1}$$

Studies on the diffusion of several labeled dextrans, Ficolls and proteins of different size and charge in the cytoplasm of different cells [25–30] have shown their translational mobility to be hindered in a size-dependent manner with respect to their diffusion in aqueous buffer. Comparative translational diffusion studies of a series of globular proteins and dextrans in the same cultured cells [29,31] indicated that labeled dextrans diffused faster than proteins in the cytoplasm, *i.e.*, the viscosity experienced by diffusing molecules in cytoplasm, η_t (cytoplasm), appears to be a function of tracer size and tracer characteristics. Since the cell cytoplasm is a very complex environment, containing fluid medium, proteins, networks of cytoskeletal filaments, etc., *in vitro* studies conducted in well-defined solutions, in which the crowded cellular environment is mimicked by a high concentration of a macrosolute (water-soluble polymers such as dextrans and Ficolls or non-related proteins) [2], would constitute a first approach to the evaluation of macromolecular crowding effects on tracer diffusion. The diffusion of labeled Ficolls and dextrans have been carefully characterized in globular protein solutions of concentration comparable to the range reported for cytoplasm, by fluorescence recovery after photobleaching (FRAP) techniques [25,26]. These studies showed that the diffusion of these water-soluble polymers in concentrated solutions of globular proteins presented weaker tracer size dependence, in the opposite direction than observed in cytoplasm (dextrans diffusion), or not significantly size dependence (Ficoll diffusion), suggesting that the high protein content is not alone responsible for the observed diffusion behavior in cytoplasm. Muramatsu and Minton [32] studied the diffusion of tracer proteins in solutions crowded with proteins *via* measurements of boundary spreading, a macroscopic technique based on absorbance measurements [33]. They showed that the fractional reduction of the diffusion of the tracer increased with increasing size of tracer species, and with decreasing size of background species. On the other hand, in a recent FCS tracer diffusion study in solutions crowded with Ficoll-70 (0–60 wt.%), Dauty and Verkman [34] have found comparable percentage reductions in the translational diffusion of small solutes, proteins, DNAs, dextrans and nanospheres for each Ficoll concentration, suggesting that the relative reduction of tracer diffusion in Ficoll-70 solutions is not size-dependent. In addition, absorption anisotropy and FCS studies of different tracer globular proteins in solutions crowded with dextrans [35,36] showed that the local rotational and translational viscosities were a complex function of the size of both the tracer and the crowder molecules. Overall, these data indicate that the mechanism of steric hindrance to the diffusion of tracer globular proteins and soluble polymers of comparable size varies with the nature of the crowder molecule, and may be related to the different conformations they exhibit in solution. In general, globular proteins behave in water like hard spheres [37], whereas dextrans have a random coil structure with a high hydration and flexibility and Ficoll-70 molecules behave as relatively open structures rather than as hard-packed spheres in solutions at concentrations larger than 5 wt.% [38]. Recent studies have proposed that the observed size dependence on tracer mobility is an indirect indication that simple diffusion models may not apply and that diffusion dextrans diffusion in cytoplasm and protein diffusion in highly concentrated random-coil polymers and globular proteins solutions are anomalous [30,39]. It is important to note that this subdiffusive behavior was considerably weaker in protein crowder solutions (up to 350 mg ml^{-1}) than that was observed in the case of large dextrans [39].

The motivation for the present study was to provide an experimental basis for estimating the magnitude for the *local apparent viscosities* (η_t and η_r) of tracer proteins in solutions crowded with non-related proteins, to better understand *in vitro* protein interaction studies in protein crowded media. We have studied the translational diffusion of apomyoglobin (apoMb) in concentrated ribonuclease A (RNase A) and human serum albumin (HSA) solutions, using FCS. One of the advantages of this microscopic technique is the very low concentration of labeled protein required for the experiments (typically nM). HSA was selected as a crowder protein because it is the major macromolecular component in blood plasma. On the other hand, RNase A was chosen because of its heterogeneous nature [40], since heterogeneity is a notable property of *in vivo* biological systems which is frequently disregarded in the *in vitro* studies performed in model crowded solutions. We have measured the translational diffusion coefficients at different crowder concentrations relative to the corresponding values in buffer (buffer viscosity, η_0), and this ratio has been interpreted in terms of relative local translational apparent viscosities (η_t/η_0). In order to obtain a global view on the rotational and translational motions of tracer protein under the same crowded conditions, we have compared the relative translational viscosities as determined by FCS (this work) with the relative local rotational viscosities (η_r/η_0) taken from a TRFD study conducted in the same crowded solutions [15,41]. For each tracer, we have tried to correlate the local viscosities with the experimentally determined macroscopic (bulk) viscosity of the crowded solutions. In all the protein solutions studied in this work, local translational viscosity values were larger than the solution bulk viscosities, and also larger than the rotational viscosities for the same tracer protein under the same crowding conditions. Our FCS diffusion results agree well with the data of Muramatsu and Minton [32], and allowed us to propose preliminary empirical relationships for estimation of local translational and rotational viscosities in Eq. (1) directly from the determined bulk viscosity. As result, the determination of hydrodynamic changes and interactions in crowded protein solutions by means of FCS and TRFD techniques may be considerably simplified. However, further work

should be carried out to test the validity of the proposed relationships. Detailed studies on rotational and translational protein diffusion, like those described in this paper, using well characterized model crowded systems will contribute to understanding how the diffusion of relevant biomolecules in physiological media is modified by the presence of other macromolecules which occupy a substantial fraction of the total volume.

2. Materials and methods

2.1. Chemicals

Alexa-Fluor488 and Alexa-Fluor546 carboxylic acid succinimidyl esters were purchased from Molecular Probes, Inc. (Eugene, OR). Crystallized lyophilized equine skeletal muscle myoglobin (Mb), five times recrystallized bovine pancreatic RNase A, and crystallized lyophilized HSA were obtained from Sigma-Aldrich Chemie GmbH (Germany) and used without further purification. All proteins were exhaustively dialyzed against 20 mM phosphate, 150 mM NaCl, 0.1 mM EDTA, pH 7.4 (PE buffer) prior to the experiments.

2.2. Preparation and labeling of apomyoglobin

ApoMb preparation from Mb, and protein concentration determinations, were carried out essentially as described in Zorrilla et al. [15]. Covalent labeling reactions were allowed to proceed for 1 h at room temperature, at a molar ratio of fluorophore to protein of 1:1. Based on ε_m (Alexa488)= 71000 M^{-1} cm^{-1} at 495 nm, and ε_m (Alexa546)= 104,000 M^{-1} cm^{-1} at 556 nm (Molecular Probes, Inc), dye-to-protein ratios were determined to be 0.1 and 0.8 for apoMb labeled with Alexa488 (apoMb-A488) and Alexa546 (apoMb-A546), respectively.

2.3. Macroscopic viscosity

Bulk viscosities (η_m) of RNase A and HSA solutions (0–250 mg ml^{-1}) were measured at (20±0.1) °C using a calibrated Micro-Ostwald viscometer (SCHOTT-GERÄTE GmbH type No 51610, 0.43 mm capillary ϕ i.d.). Sample densities were determined by weighing different volumes of solutions of known concentration and varied from 1.0 to 1.04 (±0.005) g ml^{-1}. Standard deviations in viscosity determinations were less than 2%.

2.4. Fluorescence correlation spectroscopy

FCS measurements of apoMb-A488 and apoMb-A546 solutions containing up to 250 mg ml^{-1} of "background (crowder) proteins" (RNase A and HSA) were performed with a Zeiss-EVOTEC ConfoCor inverted confocal microscope (Jena, Germany). The 488 nm Ar-ion laser line and the 543 nm He/Ne laser line were used for excitation of samples containing apoMb-A488 and apoMb-A546, respectively. A 485±15 nm interference filter (Omega) was used to select the 488 nm excitation wavelength, and light intensity was adjusted by neutral density filters. The excitation light was reflected by appropriate dichroic filters and focused by a water immersion objective (C-Apochromat 40×, numerical aperture 1.2) into the sample.

Fluorescence emitted by the sample particles was collected by the same objective, passed through the dichroic mirror, the appropriate emission band filter (maximum transmission between 530 and 570 nm for λ_{ex}=488 nm, and between 560 and 620 nm for λ_{ex}=543 nm), and through a motor-controlled pinhole (set at a diameter of 40 μm) in the image plane to discriminate against out-of-focus signals. The fluorescence photons collected impinged on an avalanche photodiode whose signal was processed by a correlator card (ALV-5000) to obtain the autocorrelation function, $G(\tau)$ [19,20]. Measurements were carried out at (20±0.1) °C on 50 μl of sample solution per well in black, glass-bottomed 96-well plates (UniView™, Whatman). The total apoMb concentration in the solutions varied between 50 nM and 200 nM. Count rates were typically between 100–200 kHz. Around 10 autocorrelation traces were recorded for each sample. Data collection times were typically 60–120 s. Solutions containing only RNase A or only HSA were studied independently to evaluate the background contribution to the autocorrelation function $G(\tau)$. In general, concentrated protein solutions may exhibit significant background fluorescence, and in that case the measured fluorescence fluctuations are caused by both tracer and background molecules diffusing through the illuminated region.

Two different models were fitted to the experimental data. The first was a *single-component diffusion model* [42,43], which assumes only one fluorescent component and includes the time-dependent population and depopulation of the tracer triplet state. The second was a *two-species diffusion model*, which assumes two fluorescent components simultaneously in solution, the tracer (T) and the background proteins (B), plus one triplet state with common characteristics for tracer and background species. In the second model, $G(\tau)$ is represented as a weighted average of the corresponding tracer and background functions [44]:

$$G(\tau) = 1 + \frac{1-F_{\text{trip}} + F_{\text{trip}}\exp(-\tau/T_{\text{trip}})}{N(1-F_{\text{trip}})}\left(\xi_T \cdot \text{Diff}_T(\tau) + \xi_B \cdot \text{Diff}_B(\tau)\right) \quad (2)$$

where N is the total average number of fluorescent molecules in the detection volume, F_{trip} and T_{trip} are the fractional population and the relaxation time of the triplet state respectively, $\text{Diff}_i(\tau)$ is the diffusion function of species i, and ξ_i is the fractional weighting factor for the contribution of each species to the autocorrelation function:

$$\text{Diff}_i(\tau) = \frac{1}{\left(1+\frac{\tau}{\tau_i}\right)\sqrt{1+\frac{\tau}{a^2\tau_i}}}; \qquad \xi_i = \frac{f_i n_i^2}{\left(\sum_i f_i n_i\right)^2} \quad (3)$$

where τ_i ($\tau_i=\omega_{xy}^2/4D_{ti}$) is the translational diffusion time of the fluorescent species, D_{ti} is the translational diffusion coefficient,

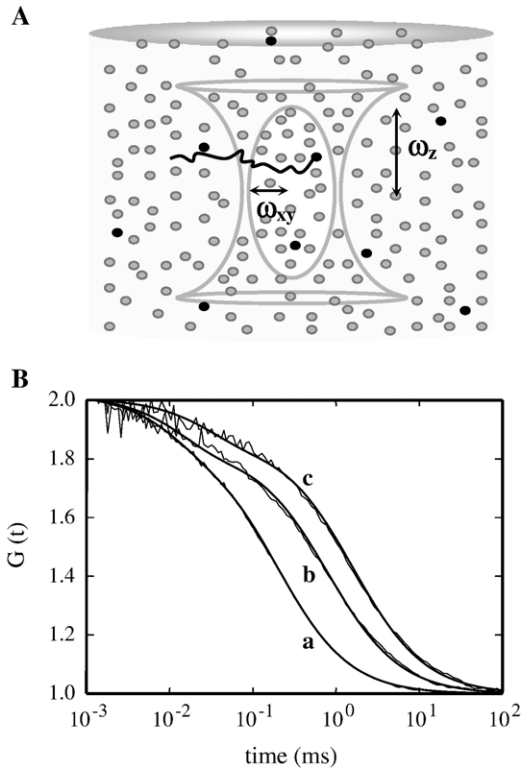

Fig. 1. FCS measurements in protein crowded solutions. (A) Schematic view of the sample volume element in an FCS experiment performed on a concentrated protein solution, with ω_z and ω_{xy} the axial and radial radii of the detection volume assumed to have a Gaussian shape in the three dimensions. Black and gray circles represent tracer-labeled apoMb and protein crowder macromolecules (HSA or RNase A), respectively. (B) Normalized autocorrelation $G(t)$ and fitted theoretical curves (smooth lines) of apoMb-A546 in buffer solution (a), in presence of 250 mg ml^{-1} of HSA (b) and in a 250 mg ml^{-1} RNase A solution (c). PE buffer, pH 7.4, T=20 °C.

a is a structural parameter of the instrumental setup $a=\omega_z/\omega_{xy}$, with ω_z and ω_{xy} the axial and radial radii of the detection volume assumed to have a Gaussian shape in the three dimensions [45], f_i is the relative molecular fraction of each species ($f_i=N_i/N$), N_i is the number of molecules of species i, n_i is the fluorescence intensity per molecule or brightness ($n_i=I_i/N_i$), and I_i is the total fluorescence intensity of species i. The translational diffusion time (τ_i) represents the average time the fluorescent species needs to diffuse over a root mean square distance ω_{xy} (Fig. 1).

Global analysis of the autocorrelation traces was performed with the program FCS Data Processor Version 1.3 (Scientific Software Technologies Centre, Department of Systems Analysis, Belarusian State University, Minsk, Belarus) [46]. The structural parameter was determined by measuring the translational diffusion of rhodamine 6G (λ_{ex}=488 nm) or tetramethylrhodamine (λ_{ex}=543 nm), and varied between 8 and 12 (assuming a diffusion coefficient of 2.8×10^{-10} m^2 s^{-1}) [19,47]. The goodness of fit was judged from the recovered χ^2 value and from inspection of the randomness of distribution of the residuals. Data error analysis was performed at the 67% confidence level.

3. Results

3.1. Tracer diffusion coefficients in diluted buffer solution

The translational diffusion coefficients of the tracer species, apoMb-A488 and apoMb-A546 at concentrations of 50–200 nM in buffer solution, in the absence of background proteins, were determined. The *single-component diffusion* model was fitted to the autocorrelation traces, the translational diffusion time of labeled apoMb recovered being (195±5) μs. The translational diffusion coefficient in buffer (D_t^0) estimated from the diffusion time of $(9\pm1)\times10^{-11}$ m^2 s^{-1}, was in good agreement with D_t^0 values previously reported for apomyoglobin monomer (apoMb-m) [48].

3.2. Tracer diffusion coefficients in crowded solutions

Translational diffusion times of apoMb-A488 and apoMb-A546 were determined in solutions containing different concentrations of RNase A and HSA (25–250 mg ml^{-1}) with an average count rate per tracer molecule of ~23 kHz (Table 1). Background solutions containing only RNase A or HSA (25–250 mg ml^{-1}) were studied under the same experimental conditions as the buffer solutions containing only labeled apoMb. Although the total background intensity relative to the labeled apoMb signal was significant in these experiments, which in the case of HSA even precluded measurements at 488-nm excitation, the count rate per crowder molecule was in all cases lower than 4 kHz (Table 1). The background diffusion times (τ_B) were determined independently for each crowder concentration by fitting the *single-component diffusion* model to the background autocorrelation traces. The tracer diffusion times (τ_T) were then determined by fitting the *two-species diffusion model* (Eq. (2)) to the autocorrelation traces of labeled apoMb in RNase A and HSA solutions (25–250 mg ml^{-1}) with the τ_B value fixed. The alternative fitting, of the *single-component diffusion* model to the labeled apoMb autocorrelation traces, under the assumption that RNase A and HSA background contributions were negligible, gave tracer translational diffusion times coincident, within experimental error, with those recovered from the fitting of Eq. (2) for two species. This comparative analysis suggests that, under our experimental conditions, the contribution of the background to the autocorrelation function may be neglected. Koppel [49] showed that, in contrast to conventional

Table 1
Fluorescence intensity (I_i) and fluorescence intensity per molecule (brightness), n_i, for apoMb (T) and the corresponding crowder background species (B) at 250 mg ml^{-1}[(a)]

Crowder	Tracer	I_T	I_B	n_T	n_B
RNase A	apoMb-A488	120	70	23	3.5
RNase A	apoMb-A546	170	14	23	3.5
HSA	apoMb-A546	100	80	23	3.0

Intensities are expressed as photon counts per second (kHz).
[(a)] In PE buffer, pH 7.4, T=20 °C. λ_{ex}=488 nm and 543 nm for apoMb-A488 and apoMb-A546 samples, respectively.
[apoMb]=20–50 nM.

fluorescence microscopy, the critical parameter in an FCS experiment is not the total counting rate, but the counting rate per fluorescent molecule (molecular brightness, n), which in the samples studied here was about 8 times higher for the tracer than for the background species. Our results show that, even when the background solutions present some incidental fluorescence correlation, the *single-component diffusion* model may nevertheless yield tracer diffusion times to a good approximation. These results may be extended to diffusion studies in any crowded media with a background contribution similar to that encountered in this work. As expected, the translational diffusion times of apoMb-A488 and apoMb-A546 in presence of RNase A were, within the error estimates, identical. In all the model crowded solutions presented in this work, the autocorrelation traces didn't show any sign of anomalous diffusion.

The translational and rotational diffusion times of apoMb species in concentrated RNase A and HSA solutions determined are presented in Fig. 2A and B. Examination of these data shows: (i) the experimental translational diffusion times of labeled apoMb relative to the diluted buffer diffusion value ($H_t=\tau_T/\tau_T^0=D_t^0/D_t$) increased with the crowder concentration; (ii) the rotational correlation times, relative to the dilute buffer values ($H_r=\phi/\phi^0=D_r^0/D_r$), of apoMb-m and apomyoglobin dimer (apoMb-d) determined in the same crowder solutions as this work [14,15], present a similar behavior, but are much less affected by the presence of the crowder molecules than the corresponding translational diffusion. Note that apoMb is a monomer in HSA solutions, whereas it self-associates in RNaseA solutions [50], forming a flexible dimer [15]. The internal rotational motions of the dimer occur in the same time-range as does the global rotation of apoMb-m. At 250 mg ml^{-1} RNase A and 10^{-4} M apoMb, all apoMb was in dimeric form, while at nM concentrations (FCS experimental conditions) apoMb was a monomer for all the solutions examined.

3.3. Bulk viscosity as a function of crowder concentration

In Fig. 2A and B, we present the macroscopic viscosities relative to the buffer viscosity ($H_m=\eta_m/\eta_0$; $\eta_0=1.03$ cP) as a function of the crowder concentration. Note that concentrated HSA solutions show a significantly lower bulk viscosity than RNase A solutions for the same mass concentration. For practical purposes, the experimental relative bulk viscosity *vs.* mass concentration dependence for both crowders was fitted by an empirical equation based on the Mooney relation [51], which does not introduce any restrictions as to the concentration of the particle or its size distribution or shape:

$$\frac{\eta_m}{\eta_0}=\exp\left(\frac{Ac}{1-Bc}\right) \tag{4}$$

where c is the crowder concentration in mg ml^{-1}. The A and B parameters from the fit were $(2.7\pm0.1)\times10^{-3}$ ml mg^{-1} and $(1.3\pm0.1)\times10^{-3}$ ml mg^{-1}, respectively for HSA solutions, and $(3.94\pm0.05)\times10^{-3}$ ml mg^{-1} and $(1.47\pm0.03)\times10^{-3}$ ml mg^{-1}, respectively for RNase A solutions. Recent analytical ultracentrifugation experiments have shown that, over the whole of the concentration range studied, HSA itself is in monomeric state, whilst RNase A exhibits weak self-association, being a mixture of monomers and trimers, monomers and tetramers, or monomers, dimers and tetramers, with a fractional abundance of RNase A tetramers (comparable in size with HSA) of about 40% at 250 mg ml^{-1} [40]. It is known that concentrated protein solutions behave as non-Newtonian fluids, and capillary-tube viscosities, though inexpensive and simple to determine, are affected by the shear rate. Consequently, there is no attempt in this work quantitatively to interpret the macroscopic viscosity values determined for these solutions. Here we employ them only as a useful comparative tool. Nevertheless, in order to compare η_m data from different laboratories, special attention has to be paid to the characteristics of the viscometers used.

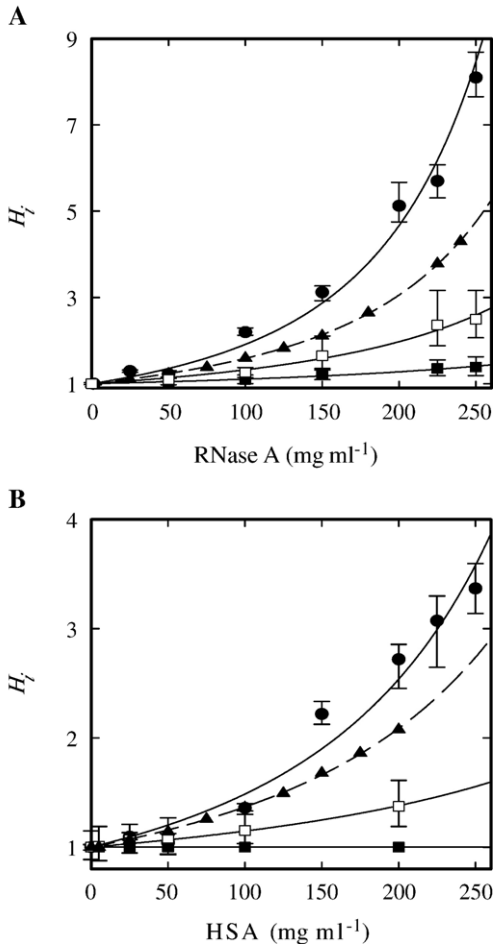

Fig. 2. Translational (●, H_{1t}), and rotational (■, H_{1r}; □, H_{2r}) diffusion times of apoMb species, and macroscopic viscosity (▲, H_m), determined in (A) concentrated RNase A and (B) HSA solutions, relative to the values observed in dilute solution, as a function of the protein crowder concentration. All translational diffusion data correspond to apoMb-m $[apoMb]_T=50$–200 nM and were obtained in work reported here. Rotational correlation time values were taken from reference [15], $[apoMb]_T=100$ μM. For the RNase A solutions, H_{2r} and H_{1r} correspond to the overall motion of apoMb-d, and to a combination of the global motion of apoMb-m and the librational motions of apoMb-d, respectively. For the HSA solutions, H_{1r} corresponds to the segmental motion of fluorescein molecules covalently attached to apoMb, and H_{2r} to the overall motion of apoMb-m, respectively. Solid lines correspond to the fit of the empirical equation $H_{t,r}=(\eta_m/\eta_0)^q$. In PE buffer, pH 7.4, at 20 °C, $\eta_0=1.03$ cP.

4. Discussion

A detailed molecular study of the effect of moderate concentrations of crowder proteins on the diffusion of a tracer protein is presented in this work. In addition, we have included in our study the experimental bulk viscosity of these solutions (η_m) as a helpful, macroscopic parameter. As we will show below, the parallel macroscopic viscosity study proposed here will allow prediction of tracer diffusion coefficients in crowded media from simple relationships, using η_m measured with an Ostwald micro-viscometer. These results are especially relevant to the interpretation of TRFD and FCS studies in physiological media.

4.1. Translational diffusion in crowded protein environments

The translational diffusion of labeled apoMb-m (tracer at nM concentration) in HSA and RNase A solutions was significantly slowed down by increasing concentrations of the crowder molecules compared to its diffusion in dilute buffer. This diffusion-retarding effect was found to be characteristic for each crowder solution (up to an 8-fold increase for 250 mg ml^{-1} RNase A solutions, and up to a 3.5-fold increase for 250 mg ml^{-1} HSA solutions, see Fig. 2). It is assumed that HSA and RNase A molecules behave as obstacles in the pathway of the tracer. The observed tracer diffusion may then be explained by a presentation of a different obstacle distribution, and consequently a different effective accessible volume, to the tracer in RNase A and HSA solutions. In this regard, it is important to note that moderately concentrated RNase A solutions are much more heterogeneous than HSA solutions (see above). Assuming that the HSA molecules and the different RNase A species are densely packed in these solutions, virtually all the cavities between adjacent RNase A tetramers would be occupied by RNase A monomers and apoMb-m molecules, while in HSA solutions the cavities, in this case only between HSA monomers, would only be occupied by apoMb-m molecules. Thus, the diffusion of an apoMb-m molecule in RNase A solutions, which would imply leaving one caged environment and entering a new one, would require extra work to make room in the new cavity, in contrast with HSA solutions where most of these cavities would be empty [41]. Of course, other effects such as non-specific crowder–crowder and tracer–crowder interactions, which will depend on the characteristics of both tracer and crowder (such as size, shape, rigidity/flexibility, charge, etc.) may also contribute to the different translational diffusion hindrance experienced by the tracer. More extended studies of translational diffusion of different tracer proteins in concentrated protein solutions need to be performed to quantify these effects.

Table 2
Parameter q values from the fit of the empirical equation $H_{t,r}=(\eta_m/\eta_0)^q$ with η_m given by Eq. (4)

Tracer	Crowder	σ[a]	q_t	q_r
apoMb-m	RNase A	4.7	1.35±0.04	(0.22±0.01)[b]
apoMb-d	RNase A	6.4	–	0.61±0.05[b]
apoMb-m	HSA	4.4	1.28±0.04	0.44±0.02[b]
Mb	BSA	4.4	1.30±0.04[c]	–
BSA	BSA	8.0	1.61±0.06[c]	–
Aldolase	BSA	12.0	1.94±0.04[c]	–
Aldolase	RNase A	13.7	5.0±0.1[c]	–

[a] σ values estimated from the hydrodynamic radius of the crowder (R_B) and tracer (R_T) molecules: $\sigma=(R_B+R_T)^3/(R_B)^3$.
[b] q_r values from rotational correlation times determined in the same crowded solutions as this work [15].
[c] q_t values estimated from translational diffusion coefficients reported by Muramatsu and Minton [32].

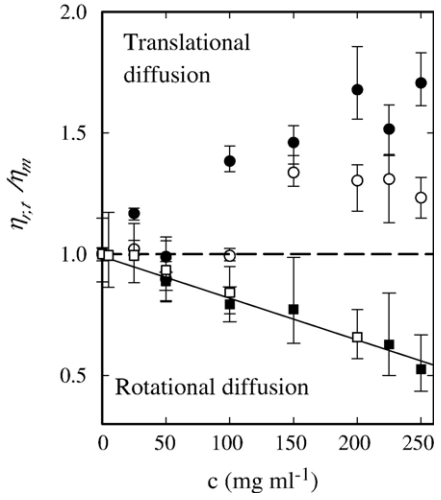

Fig. 3. Effective translational and rotational viscosities relative to macroscopic viscosity ($\eta_{r,t}/\eta_m$) as a function of protein crowder mass concentration (c). Translational viscosity of apoMb-m in RNase A (●), and HSA solutions (○), together with rotational viscosity of apoMb-m in HSA (□), and apoMb-d in RNase A solutions (■). The solid line corresponds to the fit of the empirical equation $(\eta_r/\eta_m)=1-(1.7\times10-3)\cdot c$ to the rotational diffusion data. The dashed line represents the hypothetical case for which local and macroscopic viscosity values are identical.

4.2. Effective translational and rotational viscosities vs. macroscopic viscosity

The dashed lines in Fig. 2 show the relative bulk viscosities determined for these crowded solutions ($H_m=\eta_m/\eta_0$). Assuming that there are no changes in size and/or shape of the tracer proteins with crowder concentration, and that the generalized SE and SED relations (Eq. (1)) are good approximations for diffusion studies in crowded media (see above), the relative translational and rotational diffusion times ($H_{t,r}$) determined in this and previous work [15] can be related to relative microscopic translational ($H_t=\eta_t/\eta_0$) and rotational ($H_r=\eta_r/\eta_0$) viscosities. Note that for each crowder concentration, the H_m values always fall between those of H_t and H_r. Furthermore, the average rotational correlation times associated with the global motion of apoMb-m, the domain flexibility in apoMb-d, and the segmental motion of fluorescein molecules covalently attached to apoMb [15] are all significantly less affected by the presence of crowder molecules than is the translational motion. The solid lines in Fig. 2 correspond to the fit of the empirical equation:

$$H_{t,r} = (\eta_m/\eta_0)^q \quad (5)$$

to the $H_{t,r}$ data obtained by replacing the experimental macroscopic viscosity values (η_m) by the function defined in Eq. (4) (with A and B parameters fixed). The q values determined from the fit are presented in Table 2. A similar approach has been used previously for comparable NMR, absorption anisotropy rotational and FCS translational diffusion data [52,35,36]. In addition to the results reported in this work, we have included in Table 2 the q values estimated from translational diffusion data for different tracer/crowder pairs [32], including cyanometmyoglobin/bovine serum albumin (MbCN/BSA), analogous to the apoMb/HSA pair studied in this work.

Examination of the q values presented in Table 2 shows that: (i) in all cases q values corresponding to translational diffusion data were larger than unity, whereas those for rotational diffusion were smaller than unity, being different for each tracer/crowder pair; (ii) the q parameters for apoMb translation in HSA solutions determined in this work with the microscopic technique, FCS, were coincident within experimental error with the values estimated by Muramatsu and Minton [32] for the system MbCN/BSA *via* the macroscopic technique of boundary spreading. In FCS experiments, both (local) tracer concentration and the locations of all molecules (tracer and crowder) fluctuate. The tracer will experience many independent configurations of crowder molecules and collide many times with neighboring molecules in the cavity before it moves to a new position (estimated collision times are in the ns range) [41]. Hence, the diffusion coefficients presented here, and those determined by Muramatsu and Minton [32], would correspond to the long-time regime values. This is an important result because the effect of spatial heterogeneity on translational diffusion can only be observed from diffusion measurements performed over long times [29,53]; (iii) q values corresponding to translational diffusion of different tracers in the presence of the same crowder, increase with increasing size of the tracer; (iv) q values corresponding to translational diffusion of apoMb in RNase A and HSA solutions are quite similar, whereas those for aldolase in RNase A and HSA solutions are very different [32]. Interestingly, taking together the q values determined in this work from translational diffusion data and the estimated ones from Muramatsu and Minton data [32] (excluding the aldolase/RNase A system which presents a totally different behavior), we found that they depend linearly on the excluded volume of the tracer protein molecule per unit crowder molecule volume (or reduced covolume, σ):

$$q = F + (1-F)\sigma \tag{6}$$

with $F=0.090\pm0.003$. For moderately concentrated solutions σ may be approximated by $\sigma=(R_B+R_T)^3/(R_B)^3$, where R_B and R_T the hydrodynamic radii of the crowder and tracer molecules, respectively (see Table 2). In principle, this approach would provide a simple means of estimating q parameters and translational local apparent viscosities for protein diffusion in moderately concentrated protein solutions, where subdiffusion effects are not observed.

Finally, we have quantified the departure of the rotational and translational viscosities from the bulk viscosity by the ratio $(\eta_{t,r}/\eta_m)=H_{t,r}(\eta_0/\eta_m)$, and these values are presented in Fig. 3 as a function of the crowder mass concentration. The translational diffusion data shows that the ratio (η_t/η_m) is different for the two crowders, being higher for RNase A solutions than for HSA solutions for the same mass concentration ($c>150$ mg ml^{-1}). However, (η_r/η_m) for the overall rotation of apoMb-d in RNase A solutions and apoMb-m in HSA solutions [14,15] seems to follow the same linear dependence with c:

$$(\eta_r/\eta_m) = (1-Sc) \tag{7}$$

with $S=(1.7\pm0.1)\times10^{-3}$ ml mg^{-1}. Thus, η_r can easily be estimated simply by measuring the bulk viscosity of the protein crowded solution (η_m). The observed insensitivity of the apoMb-m and apoMb-d rotating species to the crowder characteristics may be explained by the short time-range character of the rotational diffusion of the tracers, since the rotational correlation times determined for apoMb (9–54 ns) are smaller than the crowder structural relaxation time s ($\approx$120 ns for both RNase A and HSA solutions) [54]. As a result of this, apoMb global rotational diffusion times would be expected to be less sensitive to the relatively long-term rearrangements of crowder molecule structure than translational diffusion times would be. It is clear, though, that further exploration of a greater variety of tracer/crowder systems is needed in order to establish the size limits of validity of the simple empirical relations proposed in this work, to estimate η_t and η_r from the bulk viscosities (η_m) measured with an Ostwald micro-viscometer.

Acknowledgement

This work was supported by Grants BQU/2000-1500 and SAF2003-04266 from the Spanish Dirección General de Investigación. We wish to thank Dr. R. E. Dale for the critical reading of the manuscript. S. Z. acknowledges a short stay fellowship from the Comunidad de Madrid (CAM).

References

[1] A.B. Fulton, How crowded is the cytoplasm? Cell 30 (1982) 345–347.
[2] A.P. Minton, The influence of macromolecular crowding and macromolecular confinement on biochemical reactions in physiological media, J. Biol. Chem. 276 (2001) 10577–10580.
[3] M.T. Record Jr., E.S. Courtenay, S. Cayley, H.J. Guttman, Biophysical compensation mechanisms buffering *E. coli* protein–nucleic acid interactions against changing environments, Trends Biochem. Sci. 23 (1998) 190–194.
[4] S.B. Zimmerman, S.O. Trach, Estimation of macromolecule concentrations and excluded volume effects for the cytoplasm of *Escherichia coli*, J. Mol. Biol. 222 (1991) 599–620.
[5] R.J. Ellis, Macromolecular crowding: obvious but underappreciated, Trends Biochem. Sci. 26 (2001) 597–604.
[6] A.S. Verkman, Solute and macromolecule diffusion in cellular aqueous compartments, Trends Biochem. Sci. 27 (2002) 27–33.
[7] R.J. Ellis, A.P. Minton, Cell biology: join the crowd, Nature 425 (2003) 27–28.
[8] G. Rivas, F. Ferrone, J. Herzfeld, Life in a crowded world: workshop on the biological implications of macromolecular crowding, EMBO Rep. 5 (2004) 23–27.
[9] A.P. Minton, Influence of excluded volume upon macromolecular structure and associations in 'crowded' media, Curr. Opin. Biotechnol. 8 (1997) 65–69.

[10] R.J. Ellis, Macromolecular crowding: an important but neglected aspect of the intracellular environment, Curr. Opin. Struct. Biol. 11 (2001) 114–119.
[11] M.P. Brown, C. Royer, Fluorescence spectroscopy as a tool to investigate protein interactions, Curr. Opin. Biotechnol. 8 (1997) 45–49.
[12] D.M. Jameson, S.E. Seifried, Quantification of protein–protein interactions using fluorescence polarization, Methods 19 (1999) 222–233.
[13] M.P. Lillo, O. Cañadas, R.E. Dale, A.U. Acuña, Location and properties of the taxol binding center in microtubules: a picosecond laser study with fluorescent taxoids, Biochemistry 41 (2002) 12436–12449.
[14] S. Zorrilla, G. Rivas, M.P. Lillo, Fluorescence anisotropy as a probe to study tracer proteins in crowded solutions, J. Mol. Recognit. 17 (2004) 408–416.
[15] S. Zorrilla, G. Rivas, A.U. Acuña, M.P. Lillo, Protein self-association in crowded protein solutions: a time resolved fluorescence polarization study, Protein Sci. 13 (2004) 2960–2969.
[16] P.I. Bastiaens, R. Pepperkok, Observing proteins in their natural habitat: the living cell, Trends Biochem. Sci. 25 (2000) 631–637.
[17] Ruchira, M.A. Hink, L. Bosgraaf, P.J.M. van Haastert, A.J.W.G. Visser, Pleckstrin homology domain diffusion in Dictyostelium cytoplasm studied using fluorescence correlation spectroscopy, J. Biol. Chem. 279 (2004) 10013–10019.
[18] S.A. Kim, K.G. Heinze, M.N. Waxham, P. Schwille, Intracellular calmodulin availability accessed with two-photon cross-correlation, Proc. Natl. Acad. Sci. U. S. A. 101 (2004) 105–110.
[19] M. Hink, A.J.W.G. Visser, in: W. Rettig, B. Strehmel, S. Schrader, H. Seifert (Eds.), Applied Fluorescence in Chemistry, Biology and Medicine, Springer, Heidelberg, 1999, pp. 101–118.
[20] A.J.W.G. Visser, M.A. Hink, New perspectives of fluorescence correlation spectroscopy, J. Fluoresc. 1 (1999) 81–87.
[21] A. Einstein, On the theory of the Brownian movement, Ann. Phys. (Leipz.) 19 (1906) 371–381.
[22] A. Einstein, in: R. Fürth (Ed.), Investigations on the Theory of Brownian Movement, Dover, New York, 1956.
[23] P. Debye, Polar Molecules, The Chemical Catalogue Company, New York, 1929, pp. 77–108.
[24] B. Valeur, Molecular Fluorescence, Principles and Applications, Wiley-VCH, Weinheim, Germany, 2002.
[25] K. Luby-Phelps, D.L. Taylor, F. Lanni, Probing the structure of cytoplasm, J. Cell Biol. 102 (1986) 2015–2022.
[26] K. Luby-Phelps, P.E. Castle, D.L. Taylor, F. Lanni, Hindered diffusion of inert tracer particles in the cytoplam of mouse 3T3 cells, Proc. Natl. Acad. Sci. U.S. Am. 84 (1987) 4910–4913.
[27] L. Hou, F. Lanni, K. Luby-Phelps, Tracer diffusion in F-actin and Ficoll mixtures. Toward a model for cytoplasm, Biophys. J. 58 (1990) 31–43.
[28] R. Swaminathan, C.P. Hoang, A.S. Verkman, Photobleaching recovery and anisotropy decay of green fluorescent protein GFP-S65T in solution and cells: cytoplasmic viscosity probed by green fluorescent protein translational and rotational diffusion, Biophys. J. 72 (1997) 1900–1907.
[29] M. Arrio-Dupont, G. Foucault, M. Vacher, P.F. Devaux, S. Cribier, Translational diffusion of globular proteins in the cytoplasm of cultured muscle cells, Biophys. J. 78 (2000) 901–907.
[30] M. Weiss, M. Elsner, F. Kartberg, T. Nilsson, Anomalous subdiffusion is a measure for cytoplasmic crowding in living cells, Biophys. J. 87 (2004) 3518–3524.
[31] M. Arrio-Dupont, S. Cribier, G. Foucault, P.F. Devaux, A. D'Albis, Diffusion of fluorescently labeled macromolecules in cultured muscle cells, Biophys. J. 70 (1996) 2327–2332.
[32] N. Muramatsu, A.P. Minton, Tracer diffusion of globular proteins in concentrated protein solutions, Proc. Natl. Acad. Sci. U. S. A. 85 (1988) 2984–2988.
[33] A.K. Attri, A.P. Minton, An automated method for determination of the molecular weight of macromolecules via sedimentation equilibrium in a preparative ultracentrifuge, Anal. Biochem. 133 (1983) 142–152.
[34] E. Dauty, A.S. Verkman, Molecular crowding reduces to a similar extent the diffusion of small solutes and macromolecules: measurement by fluorescence correlation spectroscopy, J. Mol. Recognit. 17 (2004) 441–447.
[35] D. Lavalette, C. Tetreau, M. Tourbez, Y. Blouquit, Microscopic viscosity and rotational diffusion of proteins in a macromolecular environment, Biophys. Chem. J. 76 (1999) 2744–2751.
[36] D. Lavalette, M.A. Hink, M. Tourbez, C. Tetreau, A.J.W.G. Visser, Proteins as microviscometers: Brownian motion revisited, Eur. Biophys. J. 35 (2006) 517–522.
[37] C. Tanford, Molecular Structure, Physical Chemistry of Macromolecules, John Wiley & Sons, New York, 1961, pp. 15–137.
[38] J.R. Wenner, V.A. Bloomfield, Crowding Effects on EcoRV Kinetics and Binding, Biophys. J. 77 (1999) 3234–3241.
[39] D.S. Banks, C. Fradin, Anomalous diffusion of proteins due to molecular crowding, Biophys. J. (2005) 2960–2971.
[40] S. Zorrilla, M. Jiménez, M.P. Lillo, G. Rivas, A.P. Minton, Sedimentation equilibrium in a solution containing an arbitrary number of solute species at arbitrary concentrations: theory and application to concentrated solutions of ribonuclease, Biophys. Chemist. 108 (2004) 89–100.
[41] S. Zorrilla, G. Rivas, M.P. Lillo, in: R.M. Kamp, J. Calvete, T. Choli-Papadopoulou (Eds.), Methods Proteome and Protein Analysis, Springer-Verlag, Berlin, Germany, 2004, pp. 35–48.
[42] N.L. Thompson, in: J.R. Lakowicz (Ed.), Topics in Fluorescence Spectroscopy, Plenum Press, New York, 1991, pp. 1337–1378.
[43] P. Van den Berg, J. Widengren, M.A. Hink, R. Rigler, A.J.W.G. Visser, Fluorescence correlation spectroscopy of flavins and flavoenzymes: photochemical and photophysical aspects, Spectrochim. Acta, Part A 57 (2001) 2135–2144.
[44] R. Brock, T.M. Jovin, Fluorescence Correlation Spectroscopy, in: R. Rigler, E.S. Elson (Eds.), Theory and Applications, Springer Series in Chemical Physics, Verlag, Berlin, 2001, pp. 133–161.
[45] S.R. Aragon, R. Pecora, Fluorescence correlation spectroscopy as a probe of molecular dynamics, J. Chem. Phys. 64 (1976) 1791–1803.
[46] V.V. Skakun, M.A. Hink, A.V. Digris, R. Engel, E.G. Novikov, V.V. Apanasovich, A.J.W.G. Visser, Global analysis of fluorescence fluctuation data, Eur. Biophys. J. 34 (2005) 323–334.
[47] R. Rigler, U. Mets, J. Widengren, P. Kask, Fluorescence correlation spectroscopy with high count rate and low background: analysis of translational diffusion, Eur. Biophys. J. 22 (1993) 169–175.
[48] E. Bismuto, E. Gratton, D.C. Lamb, Dynamics of ANS binding to tuna apomyoglobin measured with fluorescence correlation spectroscopy, Biophys. J. 81 (2001) 3510–3521.
[49] D.E. Koppel, Statistical accuracy in fluorescence correlation spectroscopy, Phys. Rev. Abstr. 10 (1974) 1938–1945.
[50] J. Wilf, A.P. Minton, Evidence for protein self-association induced by excluded volume. Myoglobin in the presence of globular proteins, Biochim. Biophys. Acta 670 (1981) 316–322.
[51] M. Mooney, The viscosity of a concentrated suspension of spherical particles, J. Colloid Interface Sci. 6 (1951) 162–170.
[52] Z.H. Endre, P.W. Kuchel, Viscosity of concentrated solutions and of human erythrocyte cytoplasm determined from NMR measurement of molecular correlation times. The dependence of viscosity on cell volume, Biophys. Chemist. 24 (1986) 337–356.
[53] B.P. Olveczky, A.S. Verkman, Monte Carlo analysis of obstructed diffusion in three dimensions: application to molecular diffusion in organelles, Biophys. J. 74 (1998) 2722–2730.
[54] G.H. Koenderink, H. Zhang, D.G.A.L. Aarts, M.P. Lettinga, A.P. Philipse, G. Nägele, On the validity of Stokes–Einstein–Debye relations for rotational diffusion in colloidal suspensions, Faraday Discuss. 123 (2003) 335–354.